Available online at www.sciencedirect.com
ScienceDirect
Nuclear Instruments and Methods in Physics Research A 573 (2007) 129–132
NUCLEAR INSTRUMENTS & METHODS IN PHYSICS RESEARCH Section A
www.elsevier.com/locate/nima

Hybrid pixel detector development for medical radiography

S. Midgley[a,b,*], A. Berry[a,b], N. Benci[a,b], S. Morton[a,b], D. Phillips[a,b], P. Smith[a,b], S. Troja[a], R. Lewis[a,b]

[a]*Monash Centre for Synchrotron Science, Monash University, Clayton 3800, VC., Australia*
[b]*School of Physics, Monash University, Clayton 3800, VC., Australia*

Available online 27 November 2006

Abstract

A 7-year project has been initiated to develop hybrid pixel detectors for medical radiography. Crystalline semiconductor will be bonded to a pixellated readout chip where individual integrated circuits process each event, transferring the position, energy and timing information to the data acquisition controller. Chips will be tiled to produce a large area detector, capable of energy dispersive photon counting at moderate spatial resolution. Preliminary results from studies examining the design features and operation of the device are presented.

Keywords: Hybrid pixel detector

1. Introduction

The Monash Centre for Synchrotron Science (MCSS), in conjunction with academic, federal and industrial partners, has set up a new co-operative research centre for biomedical imaging development (CRC BID), with the purpose of developing detectors and radio-pharmaceuticals. The instrumentation group within MCSS are in the early stages of developing detectors for medical, industrial, synchrotron [1] and other scientific applications. Current projects include high-purity germanium strip detectors for small animal positron emission tomography [2–4], large area position sensitive gas proportional counter systems [5] for X-ray diffraction and small-angle X-ray scattering studies, and a hybrid pixel detectors, with energy resolving capabilities, for medical radiography.

Hybrid pixel detectors offer a number of potential benefits in medical radiography. Such devices are being actively pursued [6], predominantly to exploit the photon counting ability of pixel detectors to reduce noise and hence the dose required to obtain a satisfactory radiograph.

The hybrid pixel detector under development is illustrated in Fig. 1. It comprises a crystalline semiconductor that is bump bonded to a pixellated application specific integrated circuit (ASIC) readout chip. Each ASIC channel comprises a pre-amp, shaping amp, analogue-to-digital converter (ADC), histogramming memory, a controller and compensation network to modify amplifier gains. The controller transfers energy information to increment the correct positional memory location, and communicates with adjacent pixels resolve multi-hit events due to charge sharing. Chips will be tiled to produces a large area detector, capable of energy dispersive photon counting at moderate spatial resolution. Although the principal application is medical radiography, the acquisition of multi-spectral data will also facilitate K-edge imaging of contrast agent distribution and methods of quantitative X-ray analysis (QXRA), such as bone density measurements. The detector could also be combined with a motion system to facilitate multi view data acquisition for stereoscopic imaging and tomography.

Here, we discuss conceptual plans and operational requirements for the device, outlining the big technical challenges that must be addressed during the 7-year duration of the project. Design specifications are given in Table 1.

*Corresponding author. Tel.: +61 3 9905 3693; fax: +61 3 9905 3637.
E-mail address: stewart.midgley@sync.monash.edu.au (S. Midgley).

0168-9002/$ - see front matter © 2006 Elsevier B.V. All rights reserved.
doi:10.1016/j.nima.2006.11.008

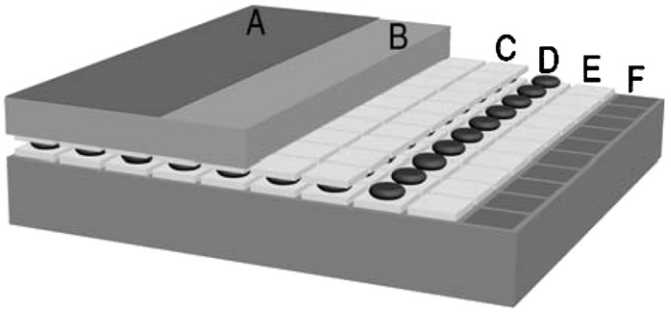

Fig. 1. Hybrid pixel detector comprising top electrode (A), pixellated semiconductor (B), collection electrodes (C), bump bonded (D) via input electrode (E) to the pixellated ASIC (F).

Table 1
Medical radiography hybrid pixel detector specifications

Mode of operation	Photon counting
Photon energy	15–25 keV (mammography and pathology) 30–120 keV (general radiography)
Area	$60 \times 30\,cm^2$
Conversion medium	Semiconductor yet to be determined
Target pixel size	$100 \times 100\,\mu m^2$
Total number of pixels	18 million
Max. count rate	50 kcps (50% dead time)
X-ray exposure times	0.02–0.05 s and longer

2. Range of photon energies and selection of the detection medium

Radiographic inspection of thin biological samples (4–8 cm thick) normally utilises W, Mo or Rh anode X-ray tubes operated at 25–35 kVp in conjunction with K-edge filtration. Samples to 30 cm thickness require harder beams, often as bremsstrahlung produced by W anode operated at 60–120 kVp. In each case, the sample absorbs the lower-energy photons and the detector must be sensitive to the spectrum of transmitted intensities: ~15–25 keV for mammography and pathology, and 30–120 keV for general radiography. Medium atomic number Z semiconductors such as Se and GaAs are suitable for mammography whilst higher Z is required for general radiography. The project will investigate the newer high Z compound semiconductor materials CdTe, $Cd_{0.9}Zn_{0.1}Te$ (CZT) and HgI_2, and explore methods for bonding these onto the readout chips.

3. Count rate requirements

Chest radiography is the most frequently performed medical examination, using film-screen as the detector. Typical exposure factors are W-anode + 3 mm Al and 110 kVp, delivering an entrance skin air KERMA of 140 μGy [7]. Using published spectral data [8], the total incident photon fluence is $3.5 \times 10^6\,ph/mm^2$, with ~1.5% transmitted through 20 cm of water. Typical exposure times are 20–500 ms, so the pixel detector needs to operate at count rates up to $10^8\,photons/s/mm^2$. For a spatial resolution of 5 line pairs/mm, the pixel size is $100 \times 100\,\mu m^2$ and the maximum count rate is 10^6 photons/s/pixel. The fabrication of each readout channel within such a small area on the ASIC chip presents significant technical challenges.

4. Energy resolution for quantitative analysis

Multi-energy data acquisition from a single exposure opens the possibility for QXRA, which delivers information about the density and composition of materials [9]. It is essential that the exponential attenuation law is obeyed; for homogeneous samples, the incident and transmitted intensities I_o and I_t are written as the ray-sum, $-\ln(I_t/I_o)$, which is proportional to thickness t. Departures from this linear relationship arise from the finite spread of energies in each bin, whereby soft X-rays are preferentially attenuated and the beam is "hardened". A feasibility study was undertaken examining beam-hardening errors for measurements with biological materials as a function of detector energy resolution, bin width and photon energy [10].

Beam-hardening calculations involved spectral attenuation of white radiation, energy blurring with a Gaussian kernel, and summation into the energy bins. The detector full width half maximum resolution ΔE was characterised by $\Delta E/E = b/\sqrt{E}$, and the bin width spanned 1–20 keV. Measured attenuation coefficients are given by

$$\mu_{expt} = \frac{1}{t}\ln\left(\sum_E I_0(E)e^{-\mu(E)t} / \sum_E I_0(E)\right)$$

which has a unique value μ_0 for zero thickness of absorber. Errors due to beam hardening $(\mu_{expt}-\mu_0)/\mu_0$ are presented in Fig. 2 as a function of photon energy and detector resolution for biological materials.

At low energies, measurements are subject to substantial errors. CZT and CdTe with measured b values 0.2–0.4 [11], deliver accurate measurement at photon energies above ~30 and 45 keV, respectively. Lower energies require higher resolution detectors (e.g., Si and Ge where $b \approx 0.1$), whilst high energies (above 100 keV) may be studied with detectors with coarse energy resolution such as NaI (where $b \geqslant 1.0$). The width of the energy integration window also introduces beam-hardening errors, especially at lower energies where it should be no larger than ΔE. Hence, at 30–100 keV, it is possible to acquire accurate measurements for QXRA using detectors with moderate energy resolution.

5. Radiographic contrast study

A simple model for the imaging chain was employed to study radiographic contrast recorded by energy integrating (EI) and photon counting (PC) detectors. The simulation incorporated energy-dependant terms for the incident W

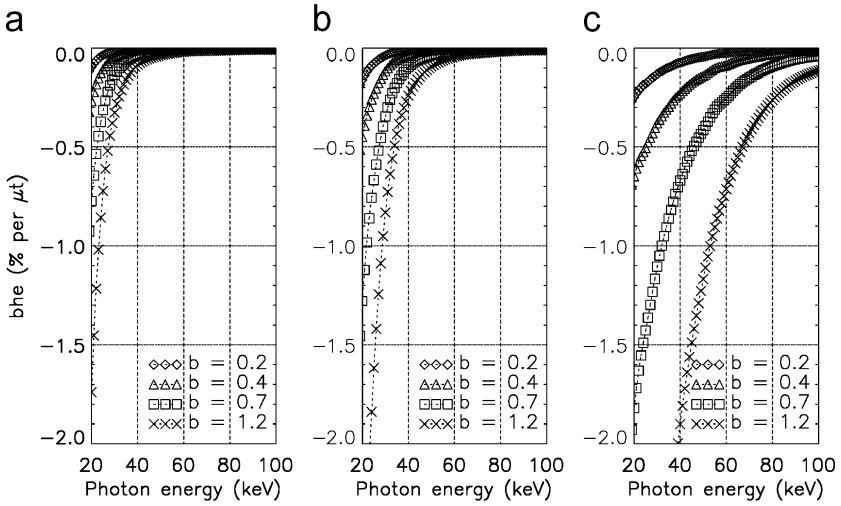

Fig. 2. Beam hardening errors using 1 keV bins for (a) lipid ($H_{98}C_{51}O_6$), (b) water and (c) bone ($H_{20}O_{26}P_5Ca_{10}$), as a function of detector energy resolution parameter b, and photon energy.

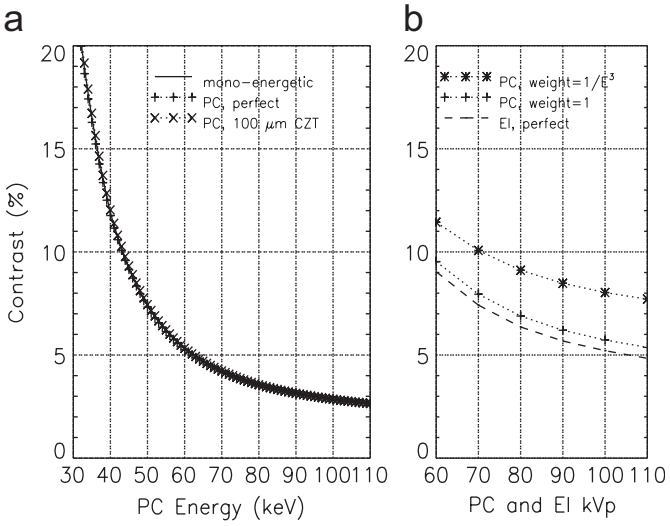

Fig. 3. Radiographic contrast for 1 mm Al in 20 cm water: (a) mono-energetic and binned PC signal, (b) total weighted PC versus total EI signal.

anode spectrum [8], filtration, attenuation by the sample [12,13] and the spectral response of the detector [14].

The target was 1 mm Al in 20 cm of water. We compared perfect detectors with unit detective efficiency and ideal PC energy resolution, against real detectors CZT and Gd_2O_2S. Results are presented in Fig. 3 where energy is the tube voltage 60–110 kVp for the total signal, and bin energy (keV) for a PC detector.

- In medical radiography, μ is propotional to $1/E^3$, so higher-energy photons interact weakly and convey low radiographic contrast. EI detectors weight according to E and over-emphasise this signal. For PC detectors with moderate energy resolution, the lower energy binned data in Fig. 3(a) exhibits improved radiographic contrast compared to the total EI signal in Fig. 3(b).
- When the influence of the detective quantum efficiency and energy resolution $b = 0.2$–0.4 are included, PC contrast is similar to that obtained from a tuneable mono-energetic X-ray source.
- The summed PC signal exhibits a small contrast improvement over the EI signal, as illustrated in Fig. 3(b).
- Weighting the PC signal according to $1/E^3$ prior to summing, delivers significant improvements in both contrast and signal-to-noise ratio (SNR) [15,16].

6. Conclusions and directions for further work

The advantages of PC operation over conventional EI detectors are:

- Additive noise sources are absent, so the image noise is quantum limited.
- Energy discrimination facilitates simultaneous multi-spectral image data acquisition from a single exposure to a poly-energetic X-ray beam.
- Binned PC data delivers improved contrast in the lower energy bins.

The device will facilitate QXRA such as bone density measurements. The principle tasks that lie ahead for the centre are:

- Development of ASIC readout chips using IBM's 90 nm fabrication process.
- Identify methods for bonding semiconductors onto the read out chips.
- Construction and acceptance testing of the prototype device.
- Development of multi-spectral data acquisition and analysis software.

Acknowledgments

This study was supported by grants from the Australian government, department for education, science and training, and the CRC for Biomedical Imaging Development.

References

[1] R. Lewis, Nucl. Instr. and Meth. A 513 (2003) 172.
[2] T. Beveridge, et al., Nucl. Instr. and Meth. A, this volume.
[3] J. Gillam, et al., Nucl. Instr. and Meth. A, this volume.
[4] P. Smith, et al., Nucl. Instr. and Meth. A, this volume.
[5] A. Berry, et al., Nucl. Instr. and Meth. A 348 (1994) 334.
[6] R.V. Kaczmarek, et al., Radiol 215 (2000) 891.
[7] Medipix collaboration, 〈http://medipix.web.cern.ch/MEDIPIX〉.
[8] J.M. Boone, J.A. Seibert, Med. Phys. 24 (1997) 1661.
[9] G. Bertuccio, Nucl Instr. and Meth. A 546 (2005) 232.
[10] S. Midgley, Rad. Phys. Chem. 75 (2006) 936–944.
[11] G.F. Knoll, Radiation Detection and Measurement, vols. 310–314, Wiley, New York, 1989 466.
[12] J.H. Hubbell, S.M. Seltzer, Tables of X-ray mass attenuation coefficients 1 keV to 20 MeV for elements $Z = 1$ to 92 and 48 additional substances of dosimetric interest, National Institute of Standards and Technology, Gaithersberg, MD, 1995.
[13] M.J. Berger, et al., XCOM: Photon Cross Section Database (version 1.2), National Institute of Standards and Technology, Gaithersberg, MD, 2005.
[14] J.Beutel, et al., Handbook of Medical Imaging, vol. 1, Physics and Psychophysics, SPIE Bellingham 200, pp. 64–176.
[15] R.N. Cahn, et al., Med. Phys. 26 (1999) 2680.
[16] D. Nieder löhner, J. Karg, J. Giersch, G. Anton, Nucl. Instr. and Meth. A 546 (2005) 37–41.